Volume 146
Number 22
21 November 2021
Pages 6671-7036

Analyst

rsc.li/analyst

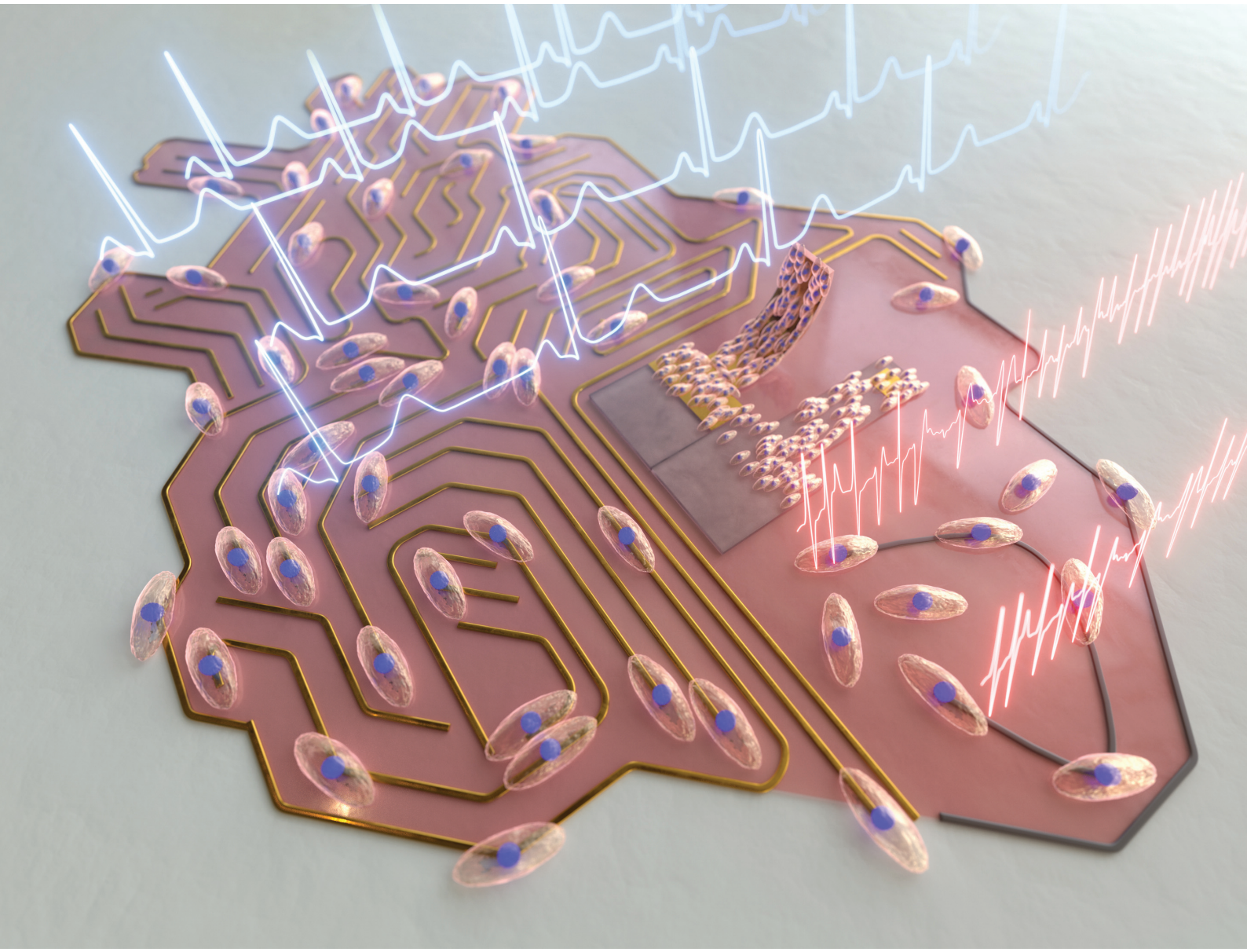

ISSN 0003-2654

ROYAL SOCIETY OF CHEMISTRY

PAPER
Dong-Weon Lee *et al.*
Enhancement of cardiac contractility using gold-coated SU-8 cantilevers and their application to drug-induced cardiac toxicity tests

Analyst

ROYAL SOCIETY OF CHEMISTRY

PAPER

View Article Online
View Journal | View Issue

Cite this: *Analyst*, 2021, **146**, 6768

Enhancement of cardiac contractility using gold-coated SU-8 cantilevers and their application to drug-induced cardiac toxicity tests†

Jongyun Kim,[a] Arunkumar Shanmugasundaram[b] and Dong-Weon Lee *[b,c,d]

Herein, we propose an array of gold (Au)-coated SU-8 cantilevers with microgrooves for improved maturation of cardiomyocytes and describe its applications to drug-induced cardiac toxicity tests. Firstly, we evaluated the effect of cell culture substrates such as polydimethylsiloxane (PDMS), polyimide (PI), and SU-8 on the cardiomyocyte's maturation. Among these, the SU-8 with microgroove structures exhibits improved cardiomyocyte maturation. Further, thin layers of graphene and Au are coated on SU-8 substrates and the effects of these materials on cardiomyocyte maturation are evaluated by analyzing the expression of proteins such as alpha-actinin, Connexin 43 (Cx43), and Vinculin. While both conductive materials enhanced protein expression when compared to bare SU-8, the Au-coated SU-8 substrates demonstrated superior cardiomyocyte maturation. The cantilever structure is constructed using microgroove patterned SU-8 with and without an Au coating. The Au-coated SU-8 cantilever showed maximum displacement of 17.6 ± 0.3 μm on day 21 compared to bare SU-8 (14.2 ± 0.4 μm) owing to improved cardiomyocytes maturation. Verapamil and quinidine are used to characterize drug-induced changes in the contraction characteristics of cardiomyocytes on bare and Au-coated SU-8 cantilevers. The relative contraction forces and beat rates changed according to the calcium and sodium channel related drugs. Matured cardiomyocytes are less influenced by the drugs compared to immature cardiomyocytes and showed reliable IC_{50} values. These results indicate that the proposed Au-coated SU-8 cantilever array could help improve the accuracy of toxicity screening results by allowing for the use of cardiomyocytes that have been matured on the drug screening platform.

Received 24th July 2021,
Accepted 26th September 2021

DOI: 10.1039/d1an01337h

rsc.li/analyst

1. Introduction

Cardiovascular disease (CVD) is the most serious life-threatening disease in contemporary culture; it claims ~18 million lives each year, accounting for 31% of all deaths.[1,2] Numerous cardiovascular drugs have been developed to date to aid in the prevention of heart attacks and strokes. Several medications, on the other hand, have been withdrawn from the market or advanced stages of preclinical drug development due to their cardiotoxic effects.[3–5] Thus, models of the cardiac musculature and methods for assessing cardiotoxicity are of great interest.

Animal models, particularly mice and rats are commonly employed as disease models in the preclinical drug development process to examine the potentially harmful effects of cardiac drugs. In drug screening and disease modeling, adult cardiomyocytes are expected to respond substantially better than immature cardiomyocytes. However, the primary cardiomyocytes are morphologically and functionally identical to fetal cells, rendering them ineffective for drug testing and disease modeling.[6,7] Therefore, the cells that can consistently reproduce characteristics of cardiovascular physiology are required to establish *in vitro* assays that investigate functional correlates of cardiac contractility, beat rate, and other elements of cardiovascular physiology.[8] To date, various techniques have been proposed to enhance cardiomyocyte maturation, including electrical, mechanical, and topographical stimulation, as well as conductive cell culture substrates. Numerous research efforts have established experimentally that electrical and/or mechanical stimulation enhances cardiomyocyte maturation

[a]*Graduate School of Mechanical Engineering, Chonnam National University, Gwangju 61186, Republic of Korea*
[b]*MEMS and Nanotechnology Laboratory, School of Mechanical Engineering, Chonnam National University, Gwangju 61186, Republic of Korea. E-mail: mems@jnu.ac.kr*
[c]*Center for Next-Generation Sensor Research and Development, Chonnam National University, Gwangju 61186, Republic of Korea*
[d]*Advanced Medical Device Research Center for Cardiovascular Disease, Chonnam National University, Gwangju 61186, Republic of Korea*
†Electronic supplementary information (ESI) available. See DOI: 10.1039/d1an01337h

during the incubation period.[9–11] However, recent studies have discovered that long-term stimulation of cardiomyocytes results in low electrophysiological signal thresholds. Additionally, when exposed to external electrical stimuli, the human ether-a-go-go related gene (hERG) and potassium (IK1) currents increased significantly.[12–16]

Cardiomyocytes show improved maturation with conductive surface, along with increased expression of connexin proteins and sarcomere length. Therefore, studies on cardiomyocytes maturation without electrical/mechanical stimulation have gained importance. Recently, positively charged polymers such as poly-D-lysine, polylysine, poly-L-ornithine, and polyethyleneimine have been used to improve cell growth and adhesion.[17–19] These positively charged polymeric materials enhance cell adhesion on culture substrates. However, polymeric substrates have undesirable side effects on cultured cells depending on their concentration, exposure time, and charge density.[20] Metal-coated substrates have also been used to increase the differentiation and maturity of cultured cells. For example, Yang *et al.* developed an electrically conductive nanofiber substrate to improve cell maturity. They fabricated nanopatterned PUA using capillary lithography and coated it with a thin layer of gold or titanium using an electron beam evaporator.[21] Kim *et al.* employed crumpled graphene to increase cell differentiation and maturity.[22] Although various materials have been shown to facilitate cell maturation, no systematic study has been conducted to evaluate the effects of cardiac drugs on the relative contraction force and contractility of cultured cardiomyocytes.

Various drug screening platforms have been developed over the years to evaluate cardiotoxicity, including patch-clamp and microelectrode array (MEA) techniques.[23–25] Patch-clamp electrophysiology remains the gold standard for studying the effects of cardiac drugs on ion channels. While patch clamps provide precise data, their low single-cell resolution and high cost preclude their use in routine laboratory conditions.[26] In comparison to patch-clamp, the MEA technique provides a higher data throughput. However, *in vitro* MEAs are less suitable due to their low spatial resolution and signal quality.[27] To investigate the effects of cardiac drugs on cells, a non-ion channel method has been proposed, such as an impedance-based cellular assay.[28,29] However, this method provides no information about the drug effect on the relative contraction force of cardiomyocytes.[30] Recently, several techniques for studying the effects of drugs on the relative contraction force and beat rate of cardiomyocytes have been proposed, including micro post,[31,32] muscular thin film,[33] and cantilever-based drug screening platforms.[34–39] Among these techniques, cantilever-based drug screening platforms have received considerable attention due to their ease of design, high accuracy, and suitability for high-throughput applications.[37]

Several polymeric cantilevers have been used in high-throughput drug screening applications to date. For instance, Kim *et al.*[34] proposed surface-patterned SU-8 cantilever arrays and investigated the adverse effects of cardiac drugs such as isoproterenol, verapamil, and astemizole on the relative contraction force and contractility of the cardiomyocyte. Oyunbaatar *et al.*[35] proposed an enhanced electromechanical stimulation of cardiac cells using a micropatterned SU-8 cantilever integrated with a metal electrode. Kim *et al.*[36] developed PI/PDMS hybrid cantilever arrays and investigated the toxicity of quinidine and verapamil to cultured cardiomyocytes. The next-generation biosensing platform based on an SU-8 based polymer cantilever array has been proposed for simultaneous measurement of electro and mechanophysiology of cardiomyocytes. While these methodologies examined the detrimental effects of cardiac drugs on the cardiomyocyte's relative contraction force and contractility in detail, they did not address cardiomyocyte maturation using conductive substrates or other pertinent research. Besides, heart muscles exhibit substantial conductive properties (0.03 to 0.6 S m^{-1}).[40] However, the substrates currently used for *in vitro* cell culture environments are not electrically conductive and do not stimulate the heart tissue microenvironment. Additionally, many scaffolds lack fibrous architectures at the low to sub-micrometer scale, which are abundant within native cardiac extracellular matrix (ECM), and play a critical role in regulating cardiac structure and function.[41]

In this study, we systematically investigated in detail the effect of various cell culture substrates such as polydimethylsiloxane (PDMS), polyimide (PI), and SU-8 on the cardiomyocyte maturation. The maturation of cardiomyocytes was then evaluated through western blot and immunocytochemical staining analysis. After preliminary experiments, SU-8 was selected as the cantilever material for measuring cardiac contractility owing to its improved maturation. For further cardiomyocyte maturation, thin conductive layers such as graphene and gold were formed on SU-8 substrate. Finally, Au-coated SU-8 cantilevers with groove structures were selected and utilized to further characterize adverse effects of cardiac drugs on cardiomyocytes contractility *in vitro*. As expected, the contractile force and beat rate of cardiomyocytes changed as a function of the drug concentration. These results indicate that mature cardiomyocytes on the proposed Au-coated SU-8 cantilever showed better drug dose response compared to immature cardiomyocytes on the non-conductive SU-8 cantilever.

2. Materials and methods

2.1. Chemicals

A commercial polystyrene based well plate was purchased from SPL Life Science Co., Ltd, Korea. Polydimethylsiloxane (PDMS) and curing agent were purchased from Dawhightech, Co., Ltd, Korea. Polyimide (PI) was purchased from Dongbaek Fine-Chem, Korea. A negative epoxy-based photoresist based on SU-8 3010, SU-8 2002, SU-8 2050 were purchased from MicroChem, USA. The monolayer graphene was purchased from the Graphenea Co. Ltd, Korea. All the materials are highly biocompatible and can be used instantly without any additional purification.

2.2. Fabrication of micro grooved cell culture substrates

To begin, a silicon (Si) master mold was used to fabricate the reusable polyurethane acrylate (PUA) mold. The Si master mold's dimensions are (3 μm in height), (3 μm in width), and (3 μm pitch distance). PUA was drop-dispensed in the calculated amount onto a Si master mold. The PUA resin was then gently pressed into contact with a 100 μm thick flexible and transparent polyethylene terephthalate (PET) support film. Following that, a uniform PUA mold was produced on the Si mold by mildly rounding the top surface of the PET film with a roller. After that, the PUA-coated Si mold was subjected to UV radiation (λ = 352 nm, 20 mJ cm^{-2}) for 10 h. The micro grooved PUA mold was gently peeled out of the Si mold after UV curing.

In a typical PDMS micro grooved fabrication process, firstly, a specified amount of PDMS was mixed in a 10 : 1 ratio with a curing agent. After that, the PDMS containing curing agent was degassed in a vacuum desiccator for 30 min to remove air bubbles. It was then spin coated at 500 rpm for 40 s on a micro grooved PUA reusable mold. The PDMS was then baked for 2 h at 80 °C on a preheated hot plate. The micro grooved PDMS substrate was lifted out of the PUA mold after the backing procedure. The micro grooved PI substrate was made using the same fabrication method as described earlier. A calculated amount of PI was spin coated on a PUA mold for 40 s at 4000 rpm. The PI was then hard backed for 1 h at 90 °C on a pre-heated hot plate. For the fabrication of SU-8 microgroove, calculated amount of SU-8 was spin coated on a Si master mold at 400 rpm for 40 s. Subsequently, the SU-8 was hard backed at 95 °C for 10 min using a pre-heated hot plate. Following the baking process, it was peeled out of the PUA mold.

2.3. Fabrication of graphene coated SU-8 substrate

Three major steps were involved in the fabrication of the monolayer graphene coated SU-8 substrate such as release, transfer and sacrificial layer removal (Fig. S1†). In a release process, slowly immerse the monolayer graphene in deionized water while separating the sacrificial layer/graphene from the support film. We removed the polymer film once the sacrificial layer/graphene is floating. To deposit monolayer graphene on the SU-8 substrate, it was submerged in deionized water and the sacrificial layer/graphene was attached from below. The SU-8 substrate with the sacrificial layer/graphene was then removed from water and dried in air for 30 min. Subsequently, the sample was baked for 1 h at 150 °C on a preheated hot plate. Then, the sample was placed in a vacuum desiccator for 24 h to prevent graphene separation from the SU-8 substrate while removing the sacrificial layer. To remove the sacrificial layer, the sacrificial layer/graphene-coated SU-8 substrate was immersed in hot acetone (50 °C) for 1 h, followed by another 1 h in iso-propyl alcohol (IPA). The sample was then dried by gentle blowing with nitrogen gas. Fig. S2a† shows the optical images of the silicon wafer with a graphene layer. As shown in Fig. S2(a and b),† a difference in the color of the graphene layer was clearly observed on a silicon dioxide layer with a thickness of 300 nm. In addition, Raman analysis also revealed the existence of graphene on the silicon wafer, as shown in Fig. S2c.†

2.4. Fabrication of gold coated SU-8 substrate

The 10/100 nm thick Cr/Au were coated on the SU-8 substrate using thermal sputtering technique. In a typical fabrication process, the SU-8 substrate was placed in a load lock chamber and then moved to a sputtering chamber. The Cr/Au deposition were carried out in a vacuum condition (5×10^{-6} Torr). The argon (Ar) gas was used to generate plasma with a flow rate of 40 sccm. The target applied power was 100 W and the pre-sputtering time was 1 min. Then, 10 nm Cr layer adhesion layer followed by 100 nm thick gold layer were deposited on a SU-8 substrate at a deposition rate of ~16.6 nm min^{-1}.

2.5. Fabrication of SU-8 cantilever

The cantilever dimension has been optimized using CATIA simulation technique. Table S1† summarize the various parameters that has been used to optimize the cantilever dimension to achieve maximum displacement. The simulation studies indicate that a cantilever with a length of 6000 μm, a width of 2000 μm, and a thickness of 15 μm is the optimal dimension for fabricating a reliable cantilever structure with a higher displacement. Fig. S3 in the ESI† shows the detailed fabrication process flow of the SU-8 cantilever. In a typical fabrication process, firstly, 300 nm thick SiO_2 sacrificial layer was formed on a 4-inch N-type (100) Si wafer using wet oxidation method (Fig S3(a and b)†). Subsequently, an 18 μm thick SU-8 3010 was spin coated at 1000 rpm for 40 s to form the cantilever structure. Then, the substrate was baked at 95 °C for 10 min flowed by UV exposure for 10 s using a mask aligner. After the UV exposure, the substrate was subjected to post exposure baking at 65 °C for 1 min and 95 °C for 4 min. Then, the sample was developed using SU-8 developer for 2 min and rinsed using IPA (Fig. S3c†). Then, 100 nm thick Au reflector was fabricated through lift-off process (AZ5214E) (Fig. S3d†). Oyunbaatar *et al.*, demonstrated that the cardiomyocytes cultured on the SU-8 substrate with 3 μm grooves exhibited a significantly enhanced α-sarcomere actinin length (~1.7 μm) compared with that of the other microgroove substrates. Therefor a ~3 μm-pitch micro groove patterns were defined on the cantilever surface using a thin SU-8 2002 (MicroChem, USA) photoresist. Typically, the SU-8 2002 was spin coated at 3000 rpm for 40 s flowed by backing at 95 °C for 2 min. Then, it was exposed to UV using a mask aligner for 5 s flowed by post exposure back at 65 °C for 1 min and 95 °C for 2 min. Next, the substrate was developed using a SU-8 developer for 1 min (Fig. S3e†). The 120 μm thick cantilever body was fabricated using SU-8 2050 photoresist. The SU-8 2050 was spin coated at 1200 rpm for 40 s followed by soft baking at 65 °C for 5 min and 95 °C for 20 min. Then, the substrate was exposed to UV using a mask aligner for 16 s. Then, the substrate was subjected to the post exposure baking process for 65 °C for 5 min and 95 °C for 10 min. Subsequently, the substrate was devel-

oped using a SU-8 developer for 9 min and rinsed by IPA (Fig. S3(f–h)†). SU-8 cantilever array was fabricated with and without gold plating to measure the cardiomyocytes contractile force according to conductive substrates. An additional Extracellular Matrix (ECM), fibronectin (Corning, 50 μg mL^{-1}) solution was coated on the surface of the SU-8 cantilever for 1 h to improve the cellular adhesion. Thereafter, the surface of the SU-8 cantilever was washed three times using phosphate Buffer Saline.

The cantilever displacement caused by the contraction and relaxation of cultured cardiomyocytes was monitored using a laser vibrometer at the free end of the SU-8 cantilever. The laser vibrometer assisted by LabVIEW was capable of measuring displacement with high accuracy, even at the nanoscale. The laser vibrometer detects light reflected from the free end of the cantilever, which is subject to frequency changes proportional to the cantilever movement. From the detected frequency shift, the software calculates the cantilever displacement. Fig. S4† shows the optical images of the array of fabricated SU-8 cantilever. The cantilever array integrated with the groove structure was used to align cardiomyocytes and was patterned with gold to enhance conductivity. A single cantilever was 6000 μm long, 2000 μm wide, 15 μm thick and a single cantilever chip consisted of 8 single cantilevers. The chips were designed to assemble in a commercial 12-well plate. Four cantilevers from a single chip were coated with a conductive material and the other 4 cantilevers were used as references to compare the relative contraction force of cardiomyocytes on an electrically conductive substrate. A reflector was placed at the bottom of the reference cantilevers to measure the relative contraction force of cardiomyocytes using a laser vibrometer.

2.6. Cell culture and neonatal rat ventricular myocytes (NRVM isolation)

The Animal Ethics Committee at Chonnam National University has approved all animal experiments. Isolation of neonatal rat ventricular myocytes (NRVM) was performed as described in our previous reports.[34] Cardiomyocytes were isolated from one day old neonatal rats (Sprague-Dawley, SD). Cardiomyocytes were isolated from cardiac tissues using an enzyme solution (Collagenase 0.4 mg mL^{-1}, Northington; Pancreatin 0.6 mg mL^{-1}, Sigma-Aldrich). The cell suspension was centrifuged using Percoll solution, and the resulting layer of fibroblasts and cardiomyocytes was separated; a high purity of cardiomyocytes was then obtained using a pre-plating method. To increase cardiomyocyte adhesion, each substrate was coated with fibronectin (50 g ml^{-1}, Corning) for 1 h. Finally, cardiomyocytes were cultured at a density of 1000 mm^{-2} on the various materials such as bare SU-8, graphene, and Au-coated SU-8. Cardiomyocytes were cultured in a conventional incubator. After 24 h, cardiomyocytes began contracting and synchronizing after 48 h.

2.7. Immunochemical staining analysis

The maturation of cardiomyocytes was determined using immunochemical staining (ICC staining) and western blot (WB) analysis. Cultured cardiomyocytes were fixed and permeabilized using paraformaldehyde (3.7%, Sigma-Aldrich) and Triton X (0.1%, Sigma-Aldrich) at 25 °C for 10 min. After 3 times washes using phosphate-buffered saline (PBS, Takara), blocking was performed with 1% bovine serum albumin (BSA, Sigma-Aldrich) for 40 min at 25 °C. After mixing the primary antibody (monoclonal anti α-sarcomere actinin and Cx43) with 1% BSA, the cells were incubated at 25 °C for 120 min. The cardiomyocytes were then incubated for 90 min at 25 °C with a mixture of secondary antibodies (Alexa-Fluor 488- or 568-labeled goat anti-mouse IgG) in 1% BSA. Finally, a solution of DAPI (4′,6-diamidino-2-phenylindole) was added for nuclear staining and incubated for 15 min at 37 °C.

3. Results and discussion

3.1. Effect of various materials on cardiomyocyte maturation

The water contact angle was measured to assess the effect of substrate characteristics on cardiomyocyte growth. Fig. S5† shows the water contact angle of various substrates based on commercial PS well plate, PDMS, PI and SU-8. A commercial PS well-plates exhibits a water contact angle of 62 ± 2.01°. The PDMS substrate was determined as a hydrophobic material with a water contact angle of 113 ± 1.85°, and PI and SU-8 were determined as hydrophilic materials with water contact angles of 76 ± 1.65° and 70 ± 2.71°, respectively. From the water contact angle, the commercial and SU-8 materials were found to be suitable for cell culture. Fig. 1b shows the scanning electron micrograph of the fabricated micro grooved SU-8 substrate. Fig. 1c optical images of the cultured cells on the micro grooved SU-8 substrate. Microscopy images of day 3 cardiomyocytes cultured on PS, PDMS, PI, and SU-8 substrates are shown in Fig. S6.† After three days of cell culture, we observed excellent cardiomyocyte attachment and synchronization on all substrates. The images in Fig. S7† depict stained cardiomyocytes cultured on a variety of substrates. Cardiomyocytes were found to grow in the microgrooves' direction.

The effect of culturing substrate and grooved on the cardiomyocytes maturation was investigated by culturing the cardiomyocytes on the different substrates such as polystyrene (PS), polydimethylsiloxane (PDMS), polyimide (PI) (Fig. 2) and SU-8. The cardiomyocytes cultured on the various substrate were periodically investigated through ICC staining analysis (Fig. S7†). Prior to determining the degree of maturation of cultured cardiomyocytes, it is necessary to understand the features utilized to measure adult cardiomyocyte maturity. The cell morphology is the most frequently investigated and used approach of maturation assessment. Although embryonic cardiac cells are quite proliferative, mature cardiomyocytes have a unique anisotropic rod form. As the cardiomyocyte grows, it enlarges its cell area and volume. Another characteristic of maturation that has been extensively investigated is the estimation of the sarcomere length and distribution of Cx43 (Cx43). The myofibrils of cardiomyocytes, which include highly structured sarcomeres, grow in length throughout maturation

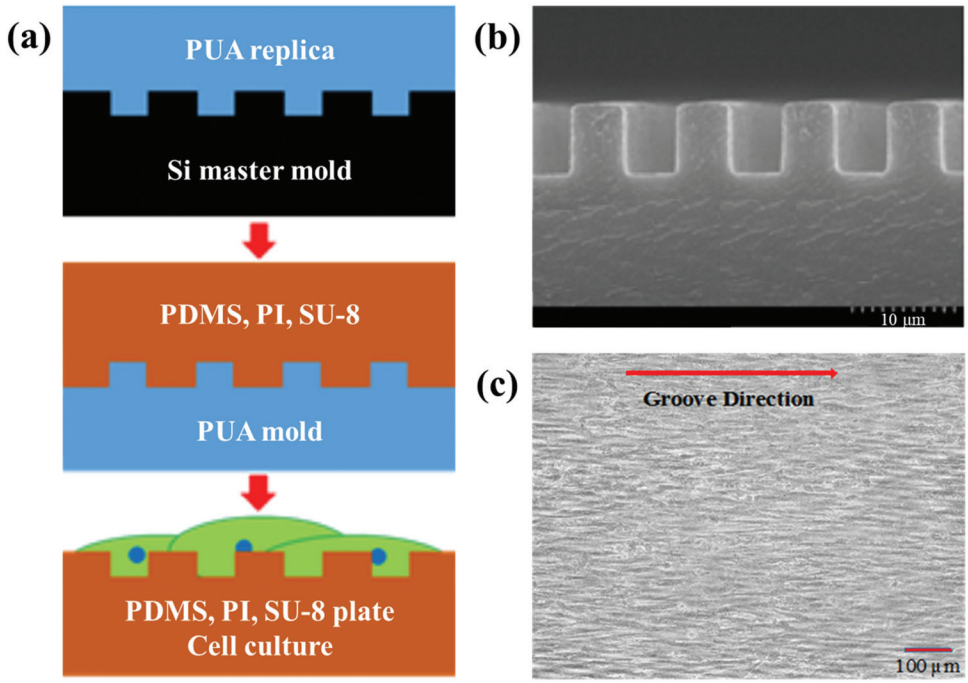

Fig. 1 (a) Fabrication of reusable PUA mold using silicon master mold. Fabrication of micro grooved PDMS, PI, SU-8 cell culture substrate using a PUA mold. (b) Scanning electron microscope image of the fabricated micro grooved SU-8 substrate. (c) Optical image of cell alignment along the direction of the microgrooves cultured on a micro grooved SU-8 substrate.

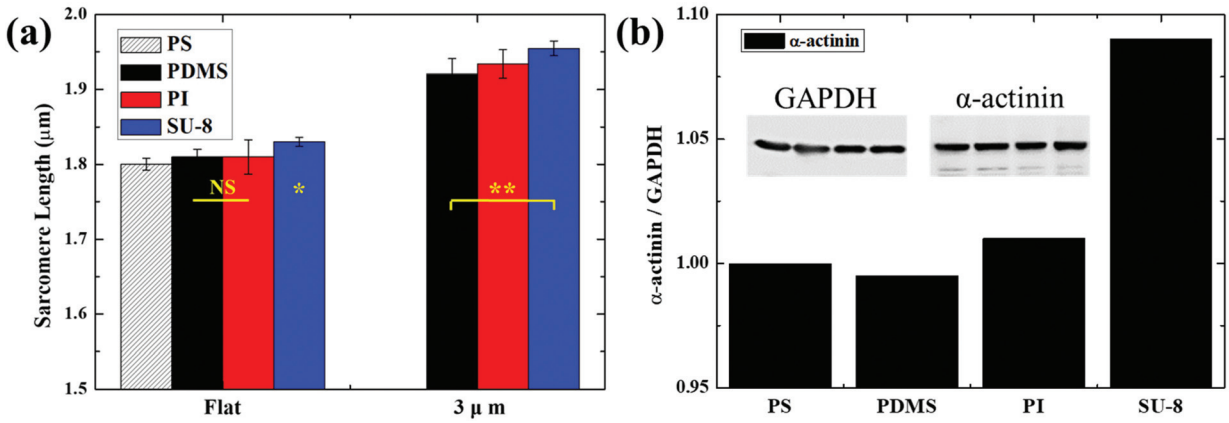

Fig. 2 Effect of culturing substrate and topography on the maturation of cardiomyocytes. (a) α-Sarcomere length of the cardiomyocytes on the cultured on the flat and grooved PDMS, PI, and SU-8. (b) α-Actinin of the cardiomyocytes on the grooved PS, PDMS, PI, and SU-8 substrates. The bars and error bars indicate the mean ± s.d., (n = 10). *P < 0.05, **P < 0.01.

and reach roughly 2.1 to 2.2 μm. The sarcomere length is determined from z line to z line, which may be determined by the expression of α-actinin. Fig. 2a shows the sarcomere length of the cultured cardiomyocytes on the flat and micro-grooved substrates. The sarcomere lengths of the cardiomyocytes cultured on the flat substrates was 1.8 ± 0.02 μm for PS, 1.81 ± 0.01 μm and 1.92 ± 0.02 μm for PDMS, 1.81 ± 0.023 μm and 1.934 ± 0.019 μm for PI, 1.83 ± 0.015 μm and 1.954 ± 0.001 μm for SU-8, respectively. Alpha actinin protein expression of the cardiomyocytes cultured on the grooved PS, PDMS, PI, and SU-8 substrates were investigated through western blot analysis (Fig. 2b). The cardiomyocytes cultured on the SU-8 substrate showed ~9% increased Alpha actinin protein expression compared to other substrates. The ICC staining and western blot analysis were demonstrating that the SU-8 substrates with microgroove structures showed better maturation could be attributed to the non-toxic, non-immunogenic and chemically inert nature. Therefore, SU-8 substrates were employed for further analysis of cardiomyocyte maturity depending on the electrical conductivity of the materials.

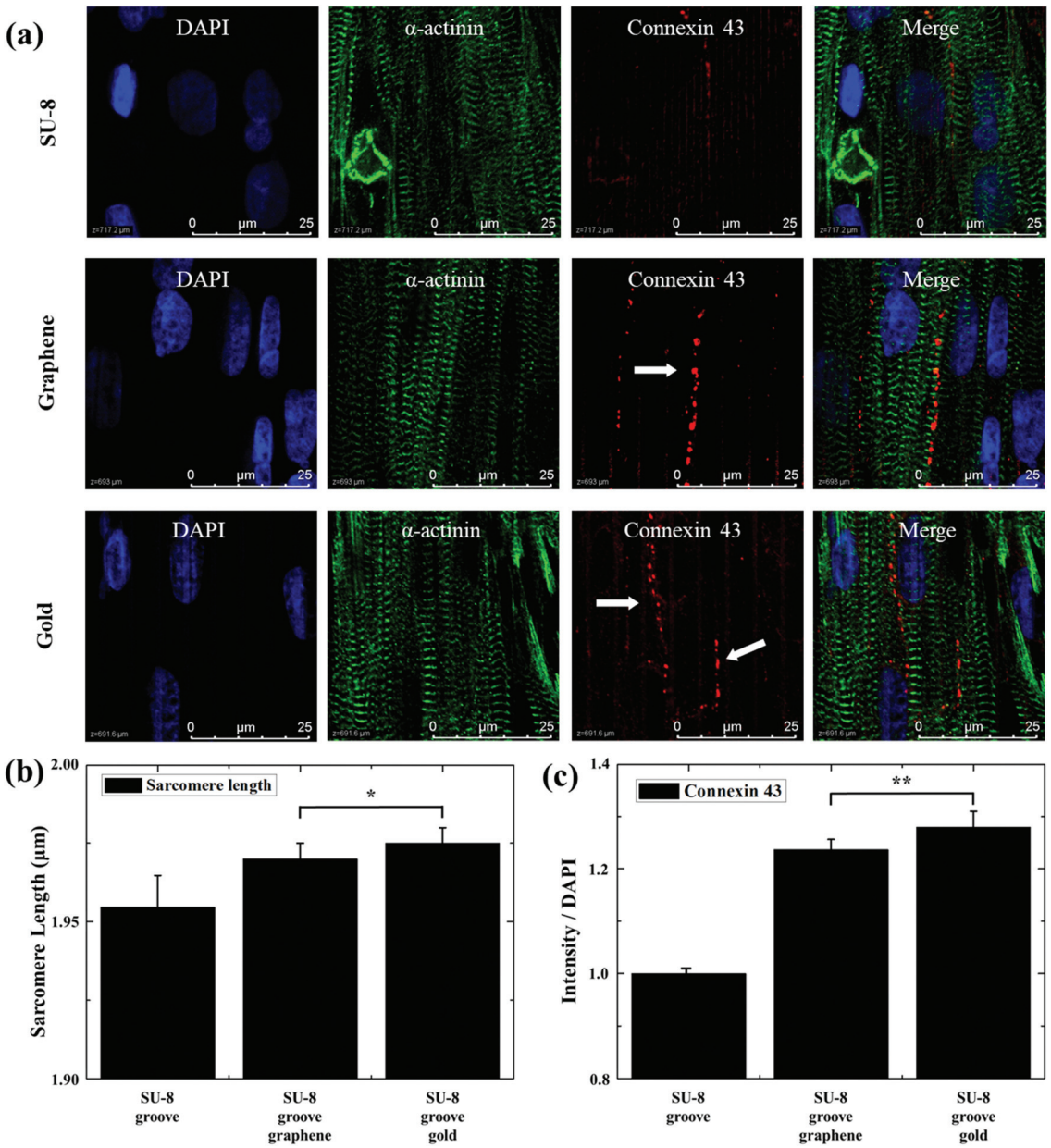

Fig. 3 Effect of electroconductive materials on the maturation of cultured cardiomyocytes. (a) ICC staining images of the cardiomyocytes cultured on the SU-8, graphene, and gold coated SU-8 substrates. (b, c) α-Sarcomere length and connection-43 of the cardiomyocytes cultured on the SU-8, graphene, and gold coated SU-8 substrates. The bars and error bars indicate the mean ± s.d., (n = 10). *P < 0.05, **P < 0.01.

3.2. Effect of electroconductive materials on the cardiomyocyte's maturation

Cardiomyocytes generated from NRVM retain an immature phenotype, which includes disorganized sarcomere structures. As a result, these cells lack the ability to create adequate anisotropic forces as adult cardiomyocytes, which reflects why they have a low response to cardiac drugs in the preclinical stage.[42] The structural organization and coordinated contraction of cultured cardiomyocytes are achieved through extensive coupling *via* gap junctions, which are multimeric intercellular channels that allow the passage of small molecules and ions between cardiomyocytes.[43] Here, we have used gold and graphene as a conductive cell culture substrate to enhance the Cx43 thereby improving the structural organization (sarcomere length) and contractility. Firstly, the effect of surface conductivity on the cultured cardiomyocytes maturation was investigated by coating different electroconductive materials such as gold and graphene on the grooved SU-8 substrate. Then, the cultured cardiomyocytes were periodically investigated using ICC staining analysis (Fig. 3a). Fig. 3a shows the fluorescence images of cardiomyocytes seeded on the bare SU-8 and graphene and gold coated SU-8 substrate.

The staining results with DAPI, alpha-actinin and Cx43 indicate the cardiomyocyte maturation status. The distinctive

anisotropic rod shape seen in the DAPI staining of cultured cardiomyocytes on grooved SU-8 and graphene and gold coated SU-8 substrates might be attributable to the topographical influence on the cultured cardiomyocytes. Fig. 3b shows the sarcomere length of cardiomyocytes cultured on the micro grooved SU-8 surface, and graphene coated, and gold coated SU-8 surface, respectively. The sarcomere length of cardiomyocytes cultured on the SU-8 surface was about 1.954 ± 0.01 μm. The values were increased up to 1.97 ± 0.005 μm on the graphene-coated SU-8 surface and 1.975 ± 0.005 μm on the gold deposited SU-8 surface, respectively. The protein expression of Cx43 by cardiomyocytes grown on the bare SU-8 surface, graphene coated, and gold SU-8 surface is shown in Fig. 3c. Cx43 is a protein that represents the gap junction intercellular communication (GJIC). This protein also indicates the cell death, proliferation, and differentiation status of cells. The Cx43 of the cardiomyocytes cultured on the SU-8 surface, graphene coated, and gold deposited SU-8 surface were about 1, 1.23 ± 0.018, and 1.28 ± 0.031, respectively. When comparing cultured cardiomyocytes on bare SU-8 and graphene coated SU-8 with gold deposited SU-8, significant improvement in the Cx43 was found on the gold deposited SU-8 surface, which indicate that gold layer can facilitate synchronized electrical signal propagation between the cells throughout the cell culture substrate.[44]

The sarcomere length and Cx43 of cultured cardiomyocytes were observed to be enhanced on the graphene coated and gold coated SU-8 surface compared to the bare SU-8 surface. However, substantial increases in sarcomere length and Cx43 were seen on Au-coated SU-8 with groove structures, indicating that the cardiomyocytes had developed. Thus, further experiments were conducted using the Au-coated substrate. Fig. S8† shows the Cx43 protein expression with and without Au layers on the SU-8 substrate. SU-8 and PS showed no significant change in Cx43 protein expression, but after gold deposition, Cx43 was increased by 2-fold. Fig. S9† shows the vinculin protein expression for cells grown on the Au-coated SU-8 substrate. Vinculin exhibits local adhesion, which was reduced by approximately 12% on the SU-8 surface compared to the PS substrates but was increased by 3% on SU-8 after coating with gold. In other words, for SU-8 substrates, vinculin protein expression increases by about 15% depending on the conductive thin film coating. The results show that cardiomyocyte adhesion was increased significantly due to the use of conductive materials such as Au. On the other hand, the incorporation of a conductive layer led to an increase in sarcomere length, and Cx43 which is consistent with earlier studies.[42–48] Finally, the Au-coated SU-8 cantilever structure with microgrooves was used to analyze the real-time relative contraction force changes of cardiomyocytes with the use of conductive materials.

3.3. Relative contraction force changes with respect to the conductive material

The obtained cardiomyocytes were cultured on the bare and Au-coated micro grooved SU-8 cantilever. Displacement of the cantilever was measured using laser vibrometer. The biocompatibility of the fabricated Au-coated SU-8 cantilever was investigated as a function of cell culture day using ICC staining analysis (Fig. S10†). Fig. 4(a and b) shows the real-time traces of cantilever displacement owing to the contractility of the cultured cardiomyocytes. The largest relative contraction force of cardiomyocytes was measured on Au-coated SU-8 cantilevers. The bar plots in Fig. 4c summarize the displacement of the micro-grooved cantilever with and without Au layer as a function of culture days. The relative contraction force increased as a function of the number of days in culture and reached the maximum on day 21 after cell seeding. The displacement of the cantilever without and with Au on culture day 7, 14, and 28 was found to be ~7.6 ± 0.5, 13.8 ± 0.3, 14.2 ± 0.4, and 14.1 ± 0.6 μm and 9.7 ± 0.2, 15.2 ± 0.5, 17.6 ± 0.3, and 17.47 ± 0.3 μm, respectively. As the days passed, cardiomyocytes matured naturally, and the cantilever displacement increased. The Au-coated SU-8 cantilever produced more displacement signifying that the cultured cardiomyocytes are more matured compared to that of bare SU-8 cantilever which was confirmed by the fluorescence staining analysis.

The staining images demonstrate that the cardiomyocytes cultured on the Au-coated SU-8 cantilever exhibits better protein expression compared to that of cultured on a bare SU-8 cantilever. Fig. 4d shows the sarcomere length of cardiomyocytes as a function of culture days. The sarcomere length of cardiomyocytes with and without the Au layer was measured every seven days as shown in Fig. 4d. The sarcomere length of cardiomyocytes was increased until day 21, slightly decreased on day 28, and then saturated. Au deposition increased the expression of alpha-actinin protein on cardiomyocytes, with significant changes in the relative contraction force and beat rate. The thin Au layer increased the cardiomyocyte relative contraction force by up to 25%; the rise time did not change much, but decay time increased by more than 500 ms, and the duration of single beating was increased with the Au layer [Table S2†]. Fig. S11† shows the characteristics of single beating of the cantilevers with and without the Au layer. Generally, the decrease in beat rate of the cardiomyocytes signifying that the cardiomyocytes are more matured.

3.4. Changes in relative contraction force with drug treatment

The adverse effects of cardiac drugs such as verapamil and quinidine on the cardiomyocytes cultured on the bare and Au-coated SU-8 cantilever. The drug was used in the experiment at various concentrations by dissolving Verapamil (L-type calcium channel blocker, Sigma-Aldrich) and Quinidine (blocking the fast-inward sodium current, Sigma-Aldrich) in ethanol. The drug concentration was prepared with different volumes of ethanol used for dilution, and all drugs used in the experiment were prepared with a concentration of 0.1% or lower. These drugs affect the different ion channels and affect the relative contraction force and contractility of the cardiomyocytes. The adverse effects of these drugs on the cultured cardiomyocytes were investigated by treating the cardiomyo-

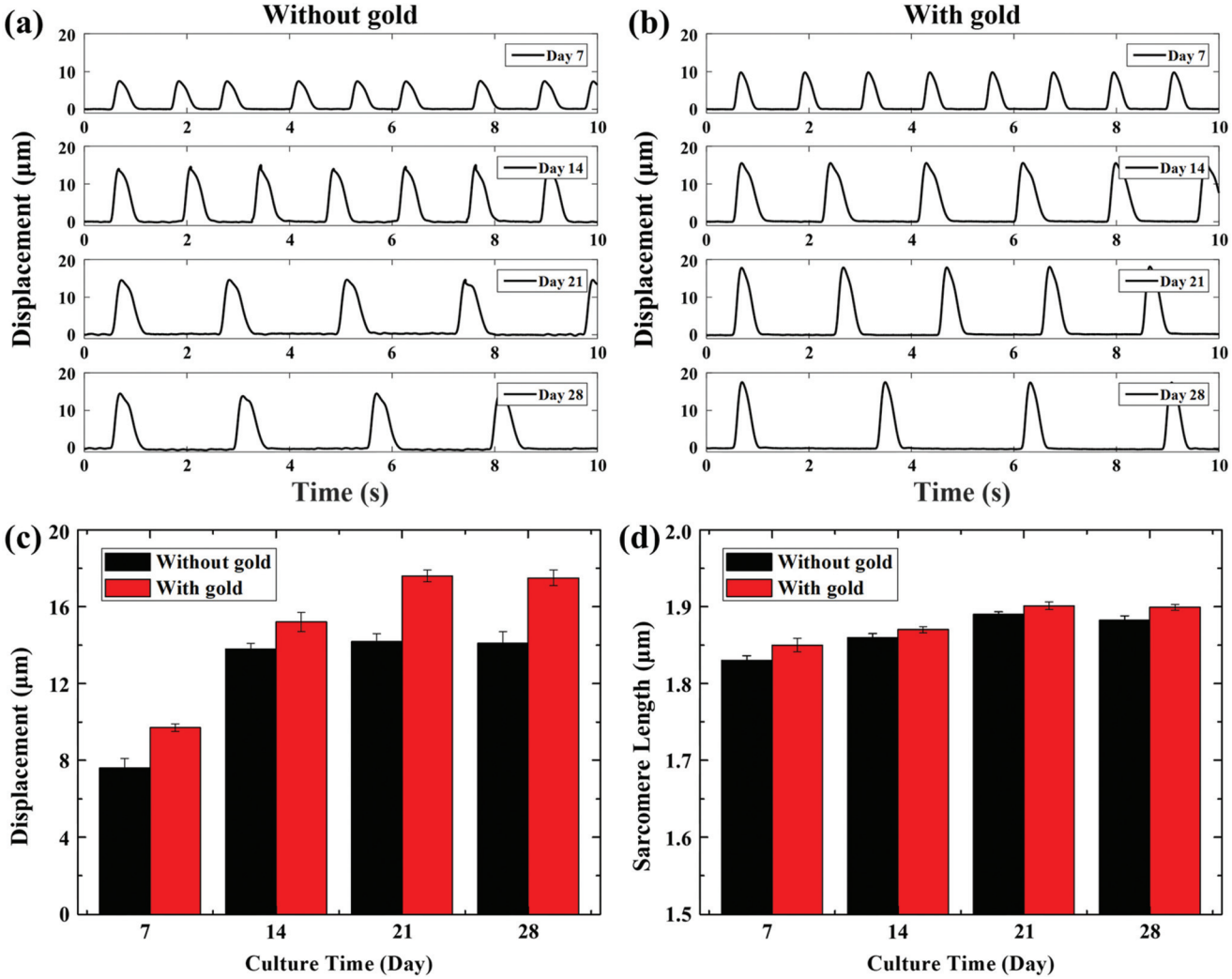

Fig. 4 Relative contraction force changes with respect to the conductive material. (a and b) Real-time traces of the cantilever displacement as a function of culture days. (c) Bar plot shows the cantilever displacement change as a function of the days in culture. (d) Changes in sarcomere length of cardiomyocytes depending on the days in culture. The bars and error bars indicate the mean ± s.d., (n = 10).

cytes with different drug concentrations. In the basic experiment, the drug concentrations of Verapamil and Quinidine were selected on a log scale based on the IC_{50} values of 136 nM and 1.068 μM, respectively. The drug concentrations were reconsidered from the perspective of contractile force change, and the specific concentration was chosen again based on the IC_{50} to screen for drug-induced toxicity. We also measured the contraction and relaxation characteristics of cardiomyocytes by replacing with new cultures after drug testing.

Fig. 5 shows the effect of verapamil on the cardiomyocytes cultured on the bare and Au-coated SU-8 cantilever. Fig. 5a shows the real-time traces of the cantilever displacement owing to the contraction and relaxation of the cultured cardiomyocytes. Verapamil is a calcium channel inhibitor that decreases the relative contraction and beat rate of cardiomyocytes as the drug concentration increases. At a concentration of 10 nM, the relative contraction force and beat rate of cardiomyocytes began to decrease, and cardiac arrest was measured at a concentration of 10 μM or higher. The normalized displacement of the bare and Au-coated SU-8 cantilever was found to be ~1, 0.818 ± 0.05, 0.773 ± 0.04, 0.763 ± 0.02, 0.479 ± 0.04, 0.448 ± 0.04 and 0.971 ± 0.01, 0.904 ± 0.04, 0.761 ± 0.04, 0.709 ± 0.01 and 0.609 ± 0.05 for control, 50 nM, 100 nM, 200 nM, 500 nM and 1 μM, respectively. Both the cantilever displacement increases after washout the drugs. The displacement of the bare and SU-8 cantilever was 0.405 ± 0.02, 0.965 ± 0.03, 0.971 ± 0.01 and 0.609 ± 0.05, 0.888 ± 0.02 and 0.988 ± 0.02 for immediately after washout and 24 h and 48 h, respectively. The cardiomyocytes cultured on the Au-coated SU-8 cantilever better recovered that bare SU-8 cantilever owing to the improved maturation.

The bar plot shows the relative contraction force of the cardiomyocytes cultured on the bare and Au-coated SU-8 cantilever as a function of verapamil concentrations (Fig. 5c). The

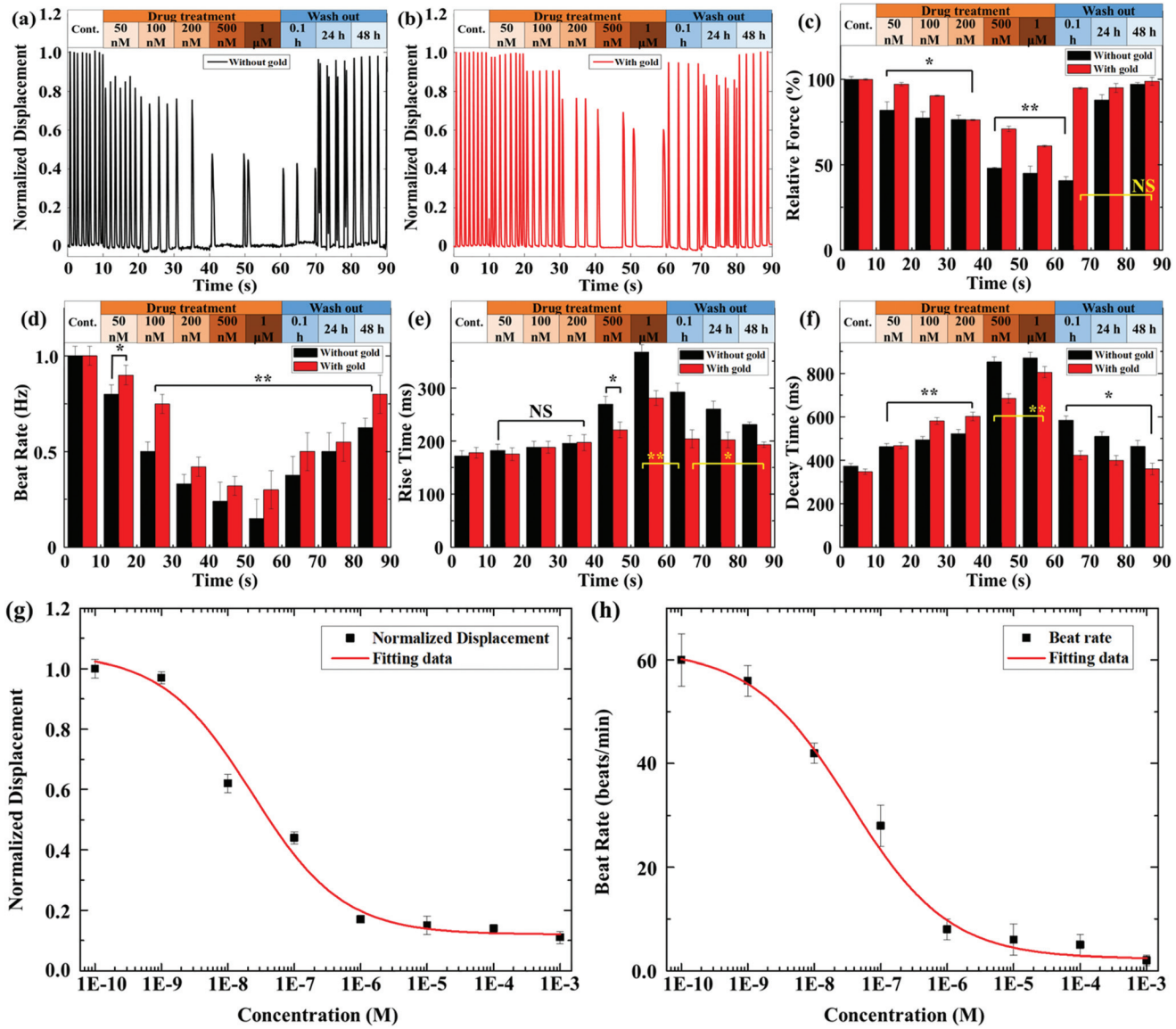

Fig. 5 Effect verapamil on the cultured cardiomyocytes. (a and b) Real-time traces of the cantilever displacement without and with Au owing to the contraction and relaxation of different concentration of verapamil treated cardiomyocytes. (c) Bar plot represents the relative contraction force of the cardiomyocytes cultured on without and with Au SU-8 cantilever as a function of different verapamil concentration. (d) Beat-rate of the cultured cardiomyocytes on the cantilever without and with Au at different drug concentration. (e and f) Rise and decay time of the cardiomyocytes at different drug concentration. (g and h) Drug dose response curve of the cardiomyocytes cultured on the Au-coated cantilever. The bars and error bars indicate the mean ± s.d., (n = 10).

relative contraction force of cardiomyocytes on bare SU-8 and Au-coated SU-8 cantilever decreased ~50% and 38% after treating the cardiomyocytes with 1 μM verapamil. The relative contraction force of cardiomyocytes cultured on the Au-coated SU-8 cantilever recovered almost to its original relative contraction force after washout the drugs whereas, the relative contraction force of cardiomyocytes on bare SU-8 cantilever recovered to its relative contraction force after 48 h wash out the drugs. Fig. 5d shows the beat rate of the cardiomyocytes on bare and Au-coated SU-8 cantilever. The beat rate of cardiomyocytes at control state was ~1 Hz. The beat rate of cardiomyocytes on bare and Au-coated SU-8 cantilever ~6.6 and 3.3 times decreased from control state after treating with 1 μM verapamil. The beat rate of the cardiomyocytes slowly recovered after washout the drug. The beat rate of the cardiomyocytes on bare SU-8 recovered ~63% whereas, it found to be ~80% on Au-coated SU-8 cantilever.

The rise of the cardiomyocytes on bare and Au-coated SU-8 cantilever at control state was ~172 ± 10 ms and 178 ± 10 ms, respectively (Fig. 5e). The rise time of the cardiomyocytes was increased with increasing drug concentration and reached maximum of 367 ± 14 ms and 281 ± 14 ms after treating the cardiomyocytes with 1 μM verapamil. Similarly, the decay time of the cardiomyocytes on both cantilevers was increased with

increasing drug concentration and reached maximum of 870 ± 25 ms and 805 ± 21 ms, respectively at 1 μM verapamil (Fig. 5f). The cardiomyocytes on Au-coated SU-8 cantilever was showed significantly better contractility behavior under the drug influence because of its better maturation than bare SU-8. Fig. 5g shows the inotropic effect of the cardiomyocytes cultured on Au-coated SU-8 cantilever. The cardiomyocytes showed negative inotropic effect that is decreased relative contraction force with increasing verapamil concentration. Fig. S10† shows the negative inotropic effect of the cardiomyocytes on bare SU-8 cantilever. Fig. 5h shows the chronotropic effect of the cardiomyocytes cultured on Au-coated SU-8 cantilever. The beat rate of the cardiomyocytes showed negative chronotropic effect that is decreased beat rate with increasing drug concentration (Fig. 5h). The IC_{50} values calculated from the inotropic effect of cardiomyocytes on bare and Au-coated SU-8 cantilever was ~80 nM (Fig. S12a†) and 122 nM (Fig. 5g), whereas the calculated IC_{50} values from the chronotropic effect were 98 nM (Fig. S12b†) and 142 nM (Fig. 5h) respectively. The cardiomyocytes cultured on the Au-coated SU-8 cantilever exhibits the same threshold IC_{50} value (136 nM) which was measured using conventional electrophysiology technique.

Fig. 6 shows the adverse effects of quinidine on the cardiomyocytes cultured on bare and Au-coated SU-8 cantilever. The changes in the relative contraction force of cardiomyocytes on SU-8 cantilever with and without the presence of a thin gold

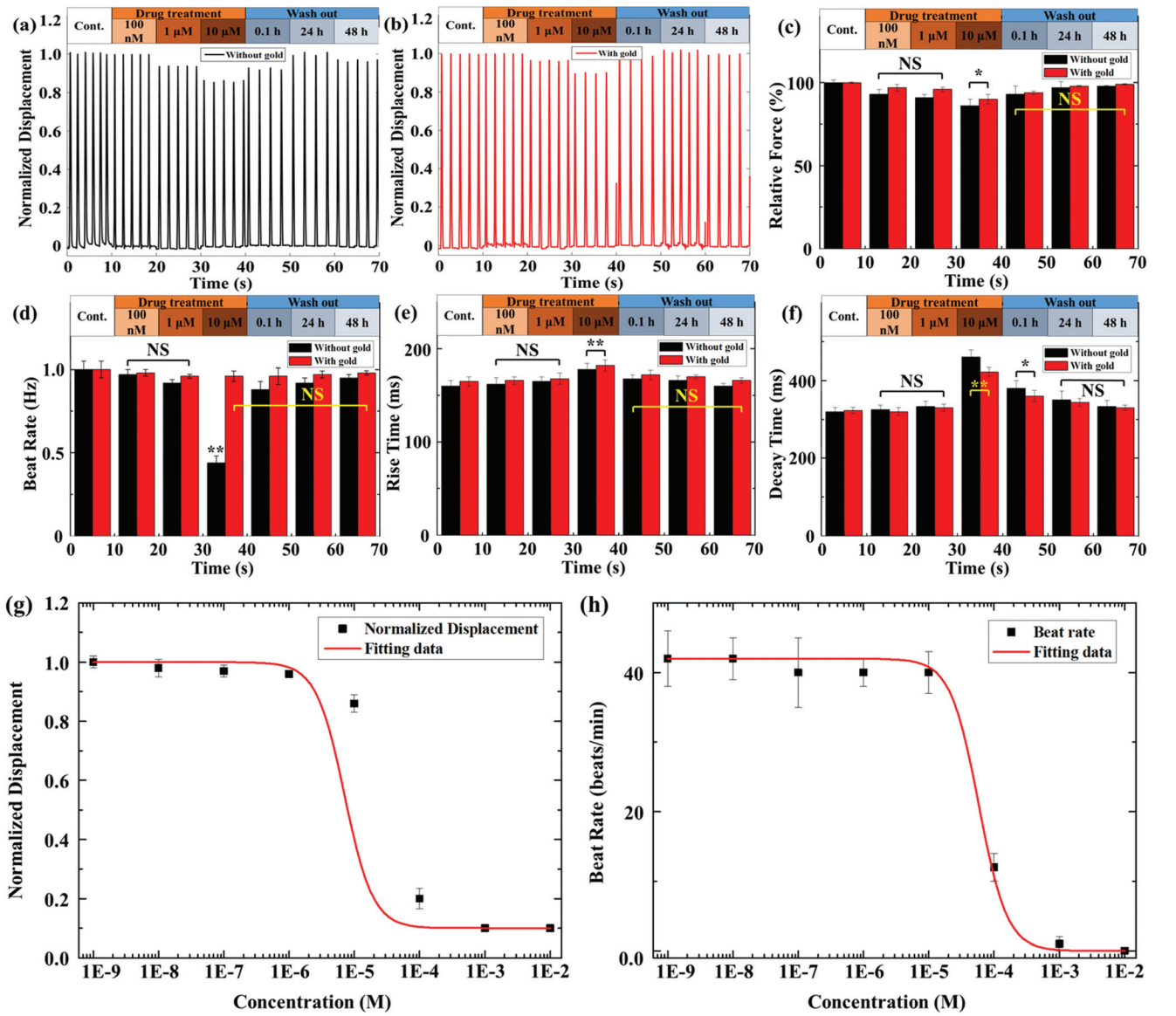

Fig. 6 Effect of quinidine on the cultured cardiomyocytes. (a and b) Real-time traces of the bare and Au-coated SU-8 cantilever displacement. (c) Relative contraction force of the cardiomyocytes cultured on bare and Au-coated SU-8 cantilever as a function of different quinidine concentration. (d) Beat-rate of the cardiomyocytes cultured on bare and Au-coated SU-8 cantilever at different drug concentration. (e and f) Rise and decay time of the cardiomyocytes at different drug concentration. (g and h) Drug dose response curve of the cardiomyocytes cultured on the Au-coated cantilever. The bars and error bars indicate the mean ± s.d., (n = 10).

film in response to quinidine was measured at specific concentration. Fig. 6(a and b) shows the normalized displacement of the cantilever due to contraction and relaxation of quinidine treated cardiomyocytes ranging from 1 nM to 10 μM. In case of the SU-8 cantilever coated with a gold film, the relative contraction force change due to the increase in drug concentration was found to be relatively small compared to the bare SU-8 cantilever. Fig. 6c shows the contractile behaviors of cardiomyocytes for a drug known as a sodium channel blocker. The relative contraction force of cardiomyocytes from 1 nM to 100 nM of quinidine was almost unchanged, but at the concentration of 1 μM they decreased strongly and at a concentration of 10 μM or higher, cardiac arrest was confirmed. The relative contraction force of the 10 μM treated cardiomyocytes on bare and Au-coated SU-8 cantilever was found to be ~32 ± 4 and 43 ± 3, respectively. The cardiomyocytes on both the cantilevers slowly recovered to their original relative contraction force after 48 h from drug washout. However, the relative contraction force of cardiomyocytes on Au-coated SU-8 cantilever showed better recovery characteristics compared to bare SU-8 cantilever.

The beat rate of the cardiomyocytes on both cantilevers did not change significantly until 1 μM but the beat rate decreased when the drug concentration was increased to 10 μM (Fig. 6d). The beat rate of the 10 μM cardiomyocytes on bare and Au-coated SU-8 film was found to be ~0.44 ± 0.04 Hz and 0.92 ± 0.02 Hz, respectively. Finally, after replacing the culture medium with fresh medium the beat rate was recovered to original beat rate. Fig. 6(e and f) shows the rise and decay time of the cardiomyocytes cultured on both the cantilevers. The rise time of the cardiomyocytes on bare and Au-coated SU-8 cantilever slightly increased to 178 ± 6 ms and 182 ± 8 ms compared their control state 160 ± 6 ms and 165 ± 2 ms. The decay time of the cardiomyocytes significantly affected at higher concentration of quinidine. Cardiomyocytes' decay times on bare and Au-coated SU-8 cantilevers were slightly increased to 320 ± 10 ms and 360 ± 15 ms, respectively, when compared to their control state values of 320 ± 12 ms and 323 ± 8 ms. The results of this experiment thus demonstrate that cardiomyocytes are irreparably damaged by the drugs above a certain concentration. Fig. 6(g and h) shows the inotropic and chronotropic effect of the cardiomyocytes cultured on Au-coated SU-8 cantilever. According to the inotropic effect of cardiomyocytes on bare and Au-coated SU-8 cantilevers, the calculated IC_{50} values were approximately 7.1 (Fig S13a†) and 8.3 μM (Fig. 6g), respectively; however, the calculated IC_{50} values according to the chronotropic effect were 6.8 (Fig. S13b†) and 7.8 μM (Fig. 6h), respectively. Both the verapamil and quinidine studies demonstrate that the cardiomyocytes cultured on Au-coated SU-8 cantilever showed better response to drugs compared to the bare SU-8 cantilever.

4. Conclusion

In this study, the cardiomyocyte maturity with conductive materials such as graphene and Au was analyzed. Cardiomyocytes showed the highest sarcomere length and alpha-actinin protein expression on the SU-8 substrate compared to other cell culture substrates. The increased sarcomere length in cardiomyocytes was measured by coating with conductive materials and cardiomyocytes maturity was confirmed by the expression of alpha-actinin, Cx43, and vinculin protein. To imitate the extracellular matrix (ECM) of actual heart tissue, the groove pattern was integrated onto the SU-8 cantilever array. The interrelationships and drug reactions of cardiomyocyte maturation and relative contraction forces under with and without the thin Au film were analyzed using SU-8 cantilever. Mature cardiomyocytes grown on an Au-coated SU-8 cantilever is more resistant to drug action than immature cardiomyocytes and show consistent IC_{50} values, which will be helpful for drug screening and other biological applications.

Author contributions

Jongyun Kim: Conceptualization; investigation; formal analysis; data curation; visualization; writing – original draft. Arunkumar Shanmugasundaram: Investigation; writing – original draft. Dong-Weon Lee: Supervised the project; funding acquisition; supervision; conceptualization; methodology; software; validation; formal analysis; data curation; visualization; writing – original draft.

Ethical statement

All animal experiments were carried out in accordance with protocols approved by Chonnam National University's Animal Ethics Committee and the Principles of Laboratory Animal Care of national laws (license number: CNU IACIC-YB-R-2015-1.

Conflicts of interest

There are no conflicts to declare.

Acknowledgements

This study was supported by a National Research Foundation of Korea (NRF) grant funded by the Korean government (MISIT) (No. 2017R1E1A1A01074550 and 2020R1A5A8018367).

References

1 G. A. Roth, *et al.*, *J. Am. Coll. Cardiol.*, 2020, **76**, 2982–3021.
2 R. Mishra and Monica, *SSM. Popul. Health*, 2019, **7**, 100365.
3 W. S. Redfern, *et al.*, *Cardiovasc. Res.*, 2003, **58**, 32–45.
4 S. Polak, M. K. Pugsley, N. Stockbridge, C. Garnett and B. Wiśniowska, *AAPS J.*, 2015, **4**, 1025–1032.

5 H. Savoji, M. H. Mohammadi, N. Rafatian, M. K. Toroghi, E. Y. Wang, Y. Zhao, A. Korolj, S. Ahadian and M. Radisic, *Biomaterials*, 2019, **198**, 3–26.
6 G.-R. Guo, L. Chen, M. Rao, K. Chen, J.-P. Song and S.-S. Hu, *J. Transl. Med.*, 2018, **16**, 288.
7 H. V. Almeida, M. F. Tenreiro, A. F. Louro, B. Abecasis, D. Santinha, T. Calmeiro, E. Fortunato, L. Ferreira, P. M. Alves and M. Serra, *ACS Appl. Bio Mater.*, 2021, **4**, 1888–1899.
8 M. Sanghavi and J. D. Rutherford, *Circulation*, 2014, **130**, 1003–1008.
9 X. Sun and S. S. Nunes, *J. Visualized Exp.*, 2017, **123**, e55373.
10 K. Ronaldson-Bouchard, S. P. Ma, K. Yeager, T. Chen, L. Song, D. Sirabella, K. Morikawa, D. Teles, M. Yazawa and G. Vunjak-Novakovic, *Nature*, 2018, **556**, 239–243.
11 K. Roshanbinfar, L. Vogt, B. Greber, S. Diecke, A. R. Boccaccini, T. Scheibel and F. B. Engel, *Adv. Funct. Mater.*, 2018, **28**, 1803951.
12 S. L. Cockerill and J. S. Mitcheson, *J. Pharmacol. Exp. Ther.*, 2006, **316**, 860–868.
13 D. Thomas, A.-B. Wimmer, K. Wu, B. C. Hammerling, E. K. Ficker, Y. A. Kuryshev, J. Kiehn, H. A. Katus, W. Schoels and C. A. Karle, *Naunyn-Schmiedeberg's Arch. Pharmacol.*, 2004, **369**, 462–472.
14 K. Jeevaratnam, K. R. Chadda, C. L.-H. Huang and A. J. Camm, *J. Cardiovasc. Pharmacol. Ther.*, 2018, **23**, 119–129.
15 N. Schmitt, M. Grunnet and S.-P. Olesen, *Physiol. Rev.*, 2014, **94**, 609–653.
16 R. Dumaine and J. M. Cordeiro, *J. Mol. Cell. Cardiol.*, 2007, **42**, 378–389.
17 Y. K. Sung and S. W. Kim, *Biomater. Res.*, 2020, **24**, 12.
18 A. Farrukh, S. Zhao and A. D. Campo, *Front. Mater.*, 2018, **5**, 62.
19 D. Smith, C. Herman, S. Razdan, M. R. Abedin, W. V. Stoecker and S. Barua, *ACS Appl. Bio Mater.*, 2019, **2**, 2791–2801.
20 K. Daliri, K. Pfannkuche and B. Garipcan, *Soft Matter*, 2021, **17**, 1156.
21 H. S. Yang, B. Lee, J. H. Tsui, J. Macadangdang, S.-Y. Jang, S. G. Im and D.-H. Kim, *Adv. Healthcare Mater.*, 2016, **5**, 137–145.
22 J. Kim, J. Leem, H. N. Kim, P. Kang, J. Choi, M. F. Haque, D. Kang and S. Nam, *Microsyst. Nanoeng.*, 2019, **5**, 53.
23 L. Sala, D. W. Oostwaard, L. G. J. Tertoolen, C. L. Mummery and M. Bellin, *J. Visualized Exp.*, 2017, **123**, e55587.
24 H. B. Hayes, *et al.*, *Sci. Rep.*, 2019, **9**, 11893.
25 S. Kussauer, R. David and H. Lemcke, *Cells*, 2019, **8**, 1331.
26 J. Gao, C. Liao, S. Liu, T. Xia and G. Jiang, *J. Nanobiotechnol.*, 2021, **19**, 97.
27 V. Viswam, M. E. J. Obien, F. Franke, U. Frey and A. Hierlemann, *Front. Neurosci.*, 2019, **13**, 385.
28 J. Stefanowicz-Hajduk and J. R. Ochocka, *Toxicol. Rep.*, 2020, **7**, 335–344.
29 J. M. Hillger, W.-L. Lieuw, L. H. Heitman and A. P. IJzerman, *Drug Discovery Today*, 2017, **22**, 1808–1815.
30 K. J. Hansen, J. T. Favreau, J. R. Gershlak, M. A. Laflamme, D. R. Albrecht and G. R. Gaudette, *Tissue Eng., Part C*, 2017, **23**, 445–454.
31 M. L. Rodriguez, B. T. Graham, L. M. Pabon, S. J. Han, C. E. Murry and N. J. Sniadecki, *J. Biomech. Eng.*, 2014, **136**, 051005-1.
32 C. A. Blair and B. L. Pruitt, *Adv. Healthcare Mater.*, 2020, **9**, e1901656.
33 A. Grosberg, A. P. Nesmith, J. A. Goss, M. D. Brigham, M. L. McCain and K. K. Parker, *J. Pharmacol. Toxicol. Methods*, 2012, **65**, 126–135.
34 J. Y. Kim, Y.-S. Choi, B.-K. Lee and D.-W. Lee, *Biosens. Bioelectron.*, 2016, **80**, 456–462.
35 N.-E. Oyunbaatar, A. Shanmugasundaram, Y.-J. Jeong, B.-K. Lee, E.-S. Kim and D.-W. Lee, *Colloids Surf., B*, 2020, **186**, 110682.
36 D.-S. Kim, Y. W. Choi, A. Shanmugasundaram, Y.-J. Jeong, J. Park, N.-E. Oyunbaatar, E.-S. Kim, M. Choi and D.-W. Lee, *Nat. Commun.*, 2020, **11**, 535.
37 J. Y. Kim, N.-E. Oyunbaatara and D.-W. Lee, *Sens. Actuators, B*, 2019, **285**, 129–136.
38 D.-S. Kim, Y.-J. Jeong, A. Shanmugasundaram, N.-E. Oyunbaatar, J. Park, E.-S. Kim, B.-K. Lee and D.-W. Lee, *Biosens. Bioelectron.*, 2021, **190**, 113380.
39 P. P. Kanade, N.-E. Oyunbaatar and D.-W. Lee, *Micromachines*, 2020, **11**, 450.
40 A. S. T. Smith, H. Yoo, H. Yi, E. H. Ahn, J. H. Lee, G. Shao, E. Nagornyak, M. A. Laflamme, C. E. Murry and D.-H. Kim, *Chem. Commun.*, 2017, **53**, 7412.
41 M. Ibrahim, *et al.*, *Hum. Mol. Genet.*, 2013, **22**, 372–383.
42 Y. Tan, D. Richards, R. Xu, S. Stewart-Clark, S. K. Mani, T. K. Borg, D. R. Menick, B. Tian and Y. Mei, *Nano Lett.*, 2015, **15**, 2765–2772.
43 M. Stahlhut, J. S. Petersen, J. K. HENNAN and M. T. Ramirez, *Cell Commun. Adhes.*, 2006, **13**, 21–27.
44 A. L. G. Mestre, *et al.*, *Sci. Rep.*, 2017, **7**, 14284.
45 P. Baei, M. Hosseini, H. Baharvand and S. Pahlavan, *J. Biomed. Mater. Res.*, 2020, **108**, 1203–1213.
46 W. E. Knight, *et al.*, *Stem Cell Rep.*, 2021, **16**, 519–533.
47 X. Yang, L. Pabon and C. E. Murry, *Circ. Res.*, 2014, **114**, 511–523.
48 J.-O. You, M. Rafat, G. J. C. Ye and D. T. Auguste, *Nano Lett.*, 2011, **11**, 3643–3648.